CrSbSe₃: A pseudo one-dimensional ferromagnetic semiconductor

Guangyu Wang ,[1,2] Lu Liu ,[1,2] Ke Yang,[3,1] and Hua Wu [1,2,4,*]

[1]*Laboratory for Computational Physical Sciences (MOE), State Key Laboratory of Surface Physics, and Department of Physics, Fudan University, Shanghai 200433, China*
[2]*Shanghai Qi Zhi Institute, Shanghai 200232, China*
[3]*College of Science, University of Shanghai for Science and Technology, Shanghai 200093, China*
[4]*Collaborative Innovation Center of Advanced Microstructures, Nanjing 210093, China*

Low-dimensional magnetic materials have attracted much attention due to their novel properties and high potential for spintronic applications. In this work, we study the electronic structure and magnetic properties of the pseudo one-dimensional compound CrSbSe₃, using density functional calculations, superexchange model analyses, and Monte Carlo simulations. We find that CrSbSe₃ is a ferromagnetic (FM) semiconductor with a band gap of about 0.65 eV. The FM couplings within each zigzag spin chain are due to the Cr-Se-Cr superexchange with the near 90° bonds, and the interchain FM couplings are one order of magnitude weaker. By inclusion of the spin-orbit coupling (SOC) effects, our calculations reproduce the experimental observation of the easy magnetization *a* axis and the hard *b* axis (the spin-chain direction), with the calculated moderate magnetic anisotropy of 0.19 meV/Cr. Moreover, we identify the nearly equal contributions from the single ion anisotropy of Cr, and from the exchange anisotropy due to the strong SOC of the heavy elements Sb and Se and their couplings with Cr. Using the parameters of the magnetic coupling and anisotropy from the above calculations, our Monte Carlo simulations yield the Curie temperature T_C of 108 K.

I. INTRODUCTION

Low-dimensional magnetic systems attract widespread attention for their novel physical properties and practical applications. Recently, two-dimensional (2D) ferromagnetism has been observed in the atomically thin layers CrI₃ and Cr₂Ge₂Te₆ [1,2], marking the beginning of a new chapter in 2D magnetism. The development of 2D magnetic materials would greatly accelerate the size reduction and promote efficiency in postsilicon microelectronics [3,4]. As the one-dimensional (1D) and 2D isotropic Heisenberg exchange systems do not have long-range magnetic order at finite temperatures, according to the Mermin-Wagner theorem [5], the emergent magnetism in low-dimensional materials should be accompanied by a magnetic anisotropy (MA). Compared to the 2D magnetic materials, a magnetic ordering is even harder to establish in 1D systems since the fluctuations become much more aggressive [6,7]. Naturally, an experimental realization of 1D FM is more challenging.

Ternary chromium trichalcogenides are a platform for low-dimensional magnets, and among them, Cr(Si, Ge)Te₃ are 2D materials of the van der Waals type, with the CrTe₆ octahedra forming a honeycomb-layered structure [2,8]. On the other hand, Cr(Sb, Ga)X_3 (X = S, Se) possess a pseudo 1D structure, in which CrX_6 octahedra form the edge-sharing double rutile chains (the zigzag Cr-spin chains) along the *b* axis and Sb or Ga atoms linking neighboring chains [9,10] (see Fig. 1). Very recently, the pseudo 1D CrSbSe₃ received a revived interest. It is a FM semiconductor with the Curie temperature

of 71 K, the band gap of 0.7 eV, and the easy magnetization *a* axis and hard *b* axis [11–13]. A recent work presented some numerical results of the structural details and a very brief description of the electronic structure and magnetism of CrSbSe₃ (and CrSbS₃), but no physical picture was discussed therein [14]. Note that in most cases, a FM material is metallic while an antiferromagnetic (AFM) one is insulating. Thus, either a FM insulator/semiconductor or an AFM metal seems to be an exception and would be of interest, let alone the low-dimensional magnetic order.

In this work, we study the electronic structure and magnetism of CrSbSe₃, using density functional calculations, superexchange model analyses, and Monte Carlo simulations. Our work finds the strongly covalent semiconducting behavior and determines the FM ground state with the easy magnetization *a* axis and hard *b* axis. The intrachain FM couplings are rationalized by the superexchange of the near-90° Cr-Se-Cr bonds (with the Se 4*p* double holes intermediate state) within the pseudo 1D zigzag spin chains, and the interchain FM couplings are one order of magnitude weaker. Moreover, we identify the single ion anisotropy of Cr and the exchange anisotropy due to the SOC of Sb 5*p* and Se 4*p* and their coupling with Cr 3*d*, and both the anisotropies are comparably moderate, being about 0.1 meV/Cr. Using the parameters of the magnetic couplings and anisotropies, our Monte Carlo simulations account for the experimental T_C.

II. COMPUTATIONAL DETAILS

Density functional calculations are carried out using the Vienna *ab initio* Simulation Package with the
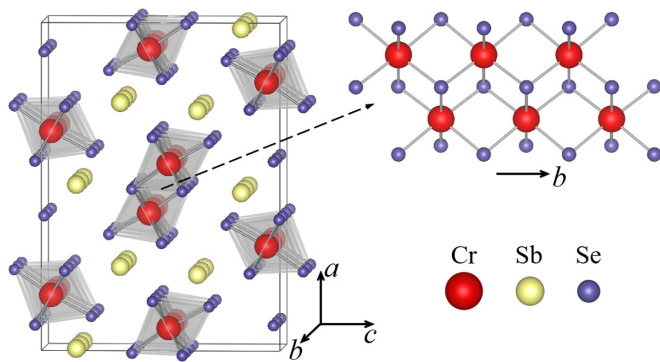
---

*Corresponding author: wuh@fudan.edu.cn

FIG. 1. The $2 \times 2 \times 1$ supercell in the pseudo 1D structure of $CrSbSe_3$ with the double rutile chains formed by the edge-sharing $CrSe_6$ octahedra, i.e., the zigzag Cr-spin chains along the b axis.

local-spin-density approximation (LSDA) [15]. The projector augmented-wave method with a plane-wave basis set is used and the cut-off energy is set to 400 eV [16]. We use the experimental lattice constants of $CrSbSe_3$ measured by single-crystal x-ray diffraction at 296 K [11], and carry out atomic relaxation until each atomic force is less than 0.01 eV/Å [the resultant Cr-Se-Cr bond lengths and angles turn out to be almost the same (within 0.4%) as the experimental ones]. A $2 \times 2 \times 1$ supercell is used, and it accommodates all the FM and AFM structures we study below. The LSDA plus Hubbard U (LSDA+U) method [17,18] is used to describe the correlation effect of the Cr $3d$ electrons, with a common value of $U = 3$ eV and Hund exchange $J_H = 1$ eV. Note that typically, U is about 3 eV for low-dimensional Cr compounds [19–21]. J_H is actually the difference of the energies of electrons with different spins or orbitals on a same atomic shell, and therefore, J_H is almost not screened and not modified when going from an atom to a solid. It is almost a constant for a given element and is typically 0.8–1.0 eV for a $3d$ transition metal [22]. As seen below, our LSDA+U calculations well reproduce the experimental semiconducting gap. The Monkhorst-Pack k-mesh of $3 \times 3 \times 2$ is sampled for integration over the Brillouin zone [23], and the $5 \times 5 \times 3$ k mesh is also tested, both showing practically the same results and ensuring a sufficient accuracy. We also include the spin-orbit coupling (SOC) in our LSDA+U+SOC calculations to study the magnetic anisotropy. Moreover, we carry out Monte Carlo simulations to estimate the Curie temperature, and the simulation details and results will be seen below.

III. RESULTS AND DISCUSSION

We first carry out the spin-constrained LDA calculation, and the obtained band structure is shown in Fig. 2. Apparently, $CrSbSe_3$ is a low-dimensional narrow-band system. In particular, a group of bands around the Fermi level arise mainly from the t_{2g} states of the Cr $3d$ orbitals, and they have the bandwidth less than 1 eV. Naturally, one expects the Coulomb correlation effects of the localized Cr $3d$ electrons.

We then perform the LSDA + U calculation to study the electronic structure of $CrSbSe_3$. Figure 3 shows the total and orbitally resolved density-of-states results in the FM state. We find that $CrSbSe_3$ has a semiconducting band gap of 0.65 eV
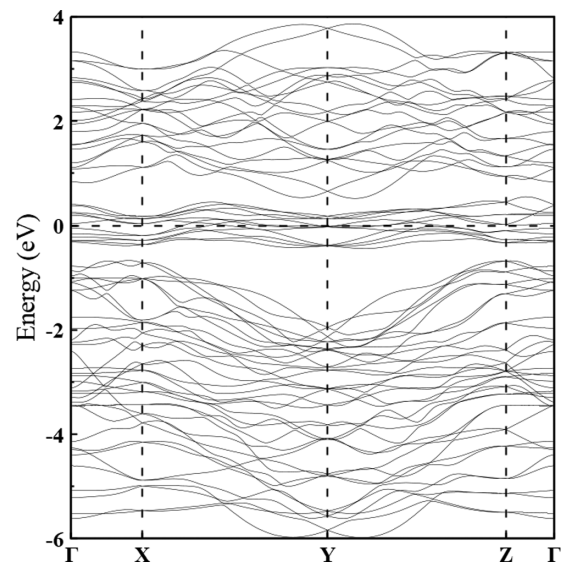

FIG. 2. Band structure of $CrSbSe_3$ by LDA: a low-dimensional narrow-band system. Fermi level is set at zero energy.

and it is in good agreement with the experimental one of 0.7 eV [11]. As the U value (here $U = 3$ eV) is much bigger than the bandwidth (less than 1 eV) of the Cr $3d$ electrons, one can name $CrSbSe_3$ a Mott-type semiconductor. The Cr $3d$ orbitals in the local $CrSe_6$ octahedral crystal field split into the lower t_{2g} triplet and higher e_g doublet. The up-spin t_{2g} orbitals are fully occupied, and the down-spin t_{2g} are empty. The higher e_g orbitals are formally unoccupied, but they seem to be partially occupied due to the strong covalence with the occupied Se $4p$ orbitals. Therefore, here the Cr ion is in the formal 3+ state and has the formal t_{2g}^3 configuration with the local spin = 3/2. The integer total spin moment of $3\mu_B$ per formula unit (f.u.) in this FM semiconducting solution agrees well with the experiments [11–13]. As the Se $4p$ and Sb $5p$ orbitals are fat ones and they have strong covalence with
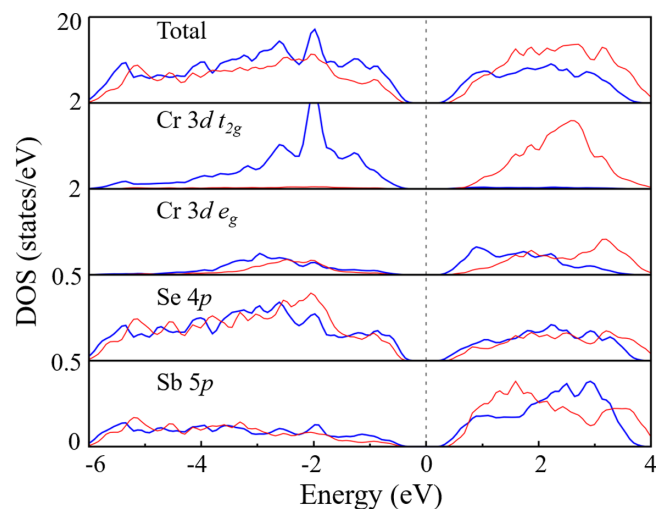

FIG. 3. Density of states (DOS) of $CrSbSe_3$ by LSDA+U: a strongly covalent Mott-type semiconductor. The blue (red) curves stand for the up (down) spin channel. Fermi level is set at zero energy.

TABLE I. Relative total energies ΔE (meV/f.u.), total spin moments M_{tot} (μ_B/f.u.), and local spin moments (μ_B) of CrSbSe₃ in different magnetic states with the a-axis magnetization by LSDA+U+SOC. The derived exchange parameters (meV) are given (see also Fig. 4; note that the far distanced intrachain $J' = -0.06$ meV is two orders of magnitude weaker than J_1 and J_2 and thus negligible). The results are also included for the FM ground state with the b- or c-axis magnetization.

States	ΔE	M_{tot}	Cr	Sb	Se
FM[a]	0.00	3.00	2.98	−0.03	−0.04
AFM1	35.85	0.00	±2.88	0.00	∓0.02
AFM2	26.43	0.00	±2.89	∓0.03	∓0.03
AFM3	0.57	0.00	±2.98	∓0.02	∓0.04
AFM4	2.26	0.00	±2.97	∓0.03	∓0.03
FM[b]	0.19	3.00	2.98	−0.03	−0.04
FM[c]	0.02	3.00	2.98	−0.03	−0.04
	J_1	J_2	J_3	J_4	
	−5.56	−4.88	−0.26	−0.50	

the Cr $3d$ orbitals, we can call CrSbSe₃ a strongly covalent Mott-type semiconductor [22,24]. Moreover, it is the Cr-Se covalence that makes the formal Se²⁻ ion have some unoccupied $4p$ components in the energy window of the unoccupied Cr $3d$ states. For this reason, the fat Se $4p$ orbitals get a minor negative spin polarization, as seen in Table I. The even fatter Sb $5p$ orbitals are also slightly spin polarized. Those strong covalences are important to the magnetic couplings and anisotropies as studied below.

We now study the magnetic structure of CrSbSe₃. To determine the magnetic ground state and the exchange parameters, we choose four different AF structures (see Fig. 4), besides the above FM state. The magnetic anisotropies are also of our concern. Therefore, here we include the SOC effects and carry out LSDA+U+SOC calculations. We define the intrachain exchange parameters J_1 and J_2 in the zigzag spin chains ($S = 3/2$), and the interchain J_3 and J_4 (see Fig. 4). Then, counting JS^2 for each spin pair, the magnetic exchange energies (per
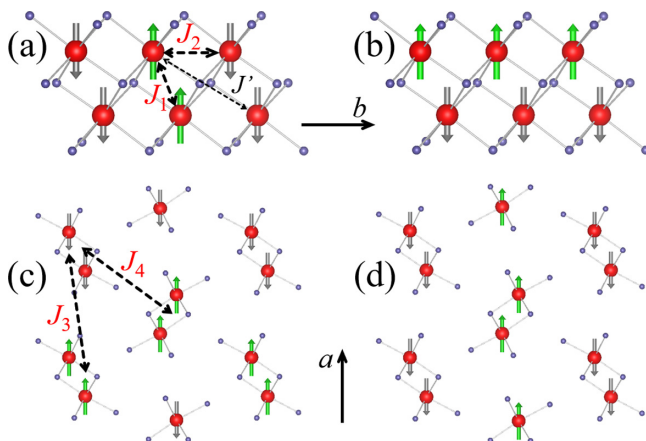

FIG. 4. The AF1/2/3/4 structures consecutively from (a) to (d). J_1 and J_2 are the exchange interactions within the zigzag chain, and J_3 and J_4 are the interchain ones. The far distanced intrachain J' turns out to be negligible.

formula unit) of the FM state and four AFM states are written as follows:

$$E_{FM} = (J_1 + J_2 + 0.5J_3 + J_4)S^2,$$
$$E_{AFM1} = -J_2S^2,$$
$$E_{AFM2} = (-J_1 + J_2)S^2,$$
$$E_{AFM3} = (J_1 + J_2 - 0.5J_3 + J_4)S^2,$$
$$E_{AFM4} = (J_1 + J_2 + 0.5J_3 - J_4)S^2.$$

As seen from the total energy results in Table I, the FM solution is the ground state. Using the values of the relative total energies and the above equations, one can derive the intrachain $J_1 = -5.56$ meV and $J_2 = -4.88$ meV, and the interchain $J_3 = -0.26$ meV and $J_4 = -0.50$ meV being one order of magnitude weaker. The far distanced intrachain J' is calculated to be -0.06 meV, and it is two orders of magnitude weaker than J_1 and J_2 and thus negligible. All this accords with the pseudo 1D structure of CrSbSe₃. All these negative values indicate that both the intra- and interchain couplings are FM. In the FM ground state, the $S = 3/2$ Cr³⁺ ion has the local spin moment of $2.98\mu_B$, and the formal Sb³⁺ and Se²⁻ ions (both having strong covalence) carry a minor negative spin moment of -0.03 and $-0.04\mu_B$. Owing to the formally closed Cr³⁺ t_{2g}^3 shell and the formal Sb³⁺ $5p^0$ and Se²⁻ $4p^6$ configurations, the SOC-induced orbital moments are marginally small, being less than $0.01\mu_B$ for each of the three elements. As a result, the total magnetic (spin) moment of $3\mu_B$/f.u. in the FM ground state (including a contribution of $0.17\mu_B$/f.u. from the interstitial region) agrees well with the experiments [11–13].

We now have a close look at the two major intrachain FM couplings J_1 and J_2, which occur between two edge-sharing CrSe₆ octahedra [see Fig. 4(a)]. This situation is similar to the extensively studied 2D material CrI₃ [25–27], whose planar honeycomb lattice is composed of the edge-sharing CrI₆ octahedra. In the insulating CrSbSe₃, the direct Cr-Cr coupling should be AFM, considering the Pauli exclusion principle in the intermediate t_{2g}^2-t_{2g}^4 state virtually excited from the t_{2g}^3-t_{2g}^3 ground state. However, the Cr-Cr distances of 3.62 Å for J_1 and 3.78 Å for J_2 are already much larger than that of 2.52 Å in the bulk Cr metal, and therefore, the direct AFM exchange should be quite weak. Instead, the near-90° Cr-Se-Cr superexchange should be dominant for both the J_1 and J_2 via the strongly covalent Cr-Se bonds. Considering the charge-transfer type band gap of CrSbSe₃, the most accessible charge excitation is from the Se $4p$ to Cr $3d$. Therefore, the virtually excited intermediate state Cr $3d^4$-Se $4p^4$-Cr $3d^4$ with the $4p$ double holes should be most plausible. Then we plot in Fig. 5 two major superexchange paths: one via the two strong $pd\sigma$ bonds (Cr $x^2 - y^2$ and Se $4p_x$ ↑) and (Se $4p_y$ ↑ and Cr $x^2 - y^2$), and the other via one strong $pd\sigma$ bond (Cr $x^2 - y^2$ and Se $4p_x$ ↑) and one moderate $pd\pi$ bond (Se $4p_x$ ↓ and Cr xy). Considering the local Hund exchange and Pauli exclusion principle [see Fig. 5(c)], both the superexchange paths give the effective Cr-Cr FM couplings within the zigzag chains.

Magnetic anisotropy is of great concern for low-dimensional magnets. Here we carry out LSDA+U+SOC calculations by assuming the different magnetization axes
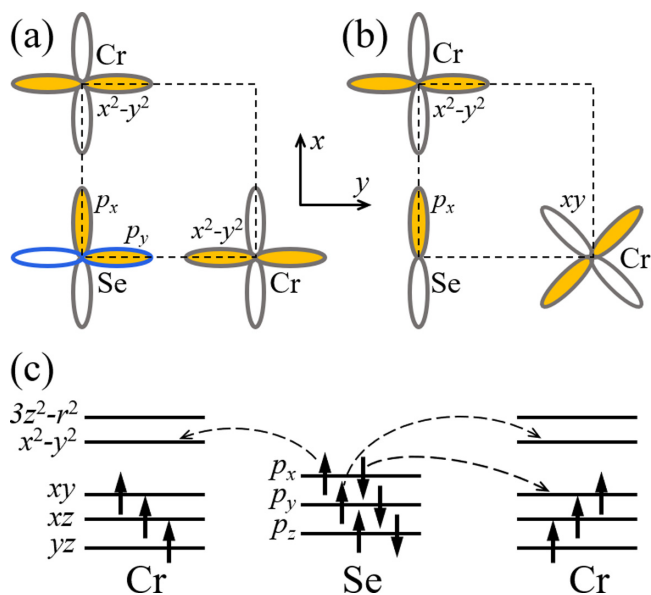
FIG. 5. (a) and (c) FM superexchange in the double rutile chains via the $(x^2 - y^2)$-(p_x, p_y)-$(x^2 - y^2)$ orbitals. (b) and (c) FM superexchange via the $(x^2 - y^2)$-p_x-xy orbitals.

within the *ab* or *ac* plane (see Fig. 1). We plot the polar diagrams of the magnetic anisotropy energy (MAE) in Fig. 6. Our results represented by the data points show that the *a* axis is the easy magnetization axis, which is perpendicular to the double rutile chains along the *b* axis. The *b* axis turns out to be the hard one with the MAE of 0.19 meV/Cr, and the *c* axis is the intermediate one with MAE of 0.02 meV/Cr relative to the easy *a* axis (see also Table I). Our finding of the easy magnetization axis reproduces the experimental observation [11,12]. Moreover, the experimental saturation magnetic fields of 0.1, 1, and 1.5 Tesla, respectively, along the *a*, *c*, and *b* axes indicate that the MAE is at the energy scale of 0.1 meV/Cr, being in agreement with our calculations.

Now we seek the origin of the MA which breaks the spin-rotational invariance. Single ion anisotropy (SIA) and exchange anisotropy (EA) are quite common in low-dimensional magnets [26–29]. The magnetic behavior of a system with strong SIA may be described by the Ising model. For example, VI_3 monolayer, out of its bulk van der Waals structure, was
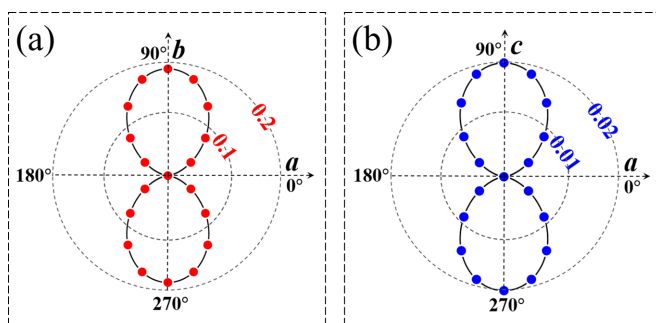

FIG. 6. Polar diagrams of the MAE in the *ab* plane (a) and the *ac* plane (b). The dashed circles with different radius represent the magnitude of MAE (in units of meV/Cr). The red and blue dots refer to the MAE values obtained in our calculations.
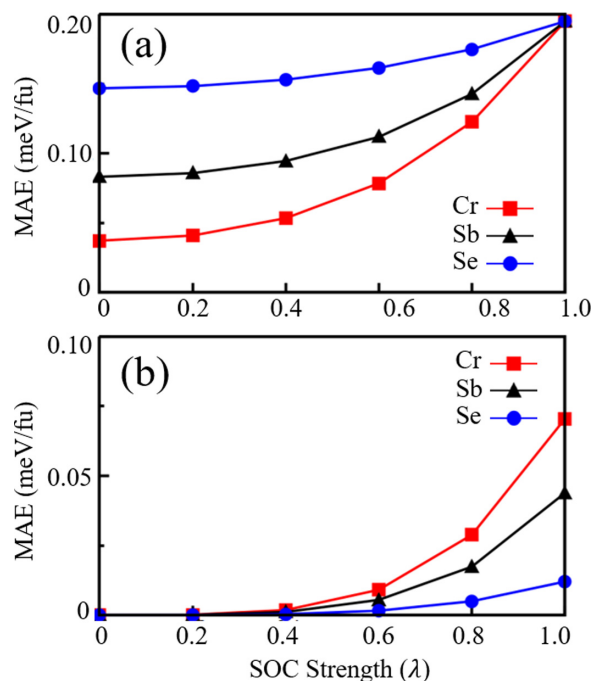

FIG. 7. (a) Red line: evolution of the MAE ($FM^b - FM^a$) as a function of λ_{Cr} while keeping λ_{Sb} and λ_{Se} at 1 (their full values). Black (blue) line: MAE as a function of λ_{Sb} (λ_{Se}) while keeping two others at 1. (b) Red line: evolution of the MAE as a function of λ_{Cr} while setting λ_{Sb} and λ_{Se} at 0. Black (blue) line: MAE as a function of λ_{Sb} (λ_{Se}) while setting two others at 0.

recently predicted to carry a large orbital moment and have a strong perpendicular SIA of about 15 meV per V^{3+} ion. In this sense, VI_3 monolayer could be a 2D Ising FM insulator [28]. The SIA arises from the intrinsic SOC effect $\lambda \vec{L} \cdot \vec{S}$, where the orbital momentum must be present (although it is quenched in many cases due to the crystal field and band formation, etc.). In $CrSbSe_3$, the formal Cr^{3+} ion has the closed t_{2g}^3 shell which seems to leave no room for orbital degree of freedom. Owing to the atomic multiplet effects and some mixture of them by the small distortion of the $CrSe_6$ octahedron, Cr^{3+} ions may have a small orbital moment and thus contribute to a small SIA.

An exchange anisotropy was proposed to be a major source of the MAE for CrI_3 [26,27]. The strong SOC of the heavy I 5p orbitals affects the FM Cr-I-Cr superexchange by the spin-orientation dependent electron hoppings, and thus yields an exchange anisotropy. In $CrSbSe_3$, the major intrachain FM couplings arise from the Cr-Se-Cr superexchange, and the weak interchain FM couplings have the contributions from the bridging Sb atoms whose 5p orbitals are more expansive. As the Se 4p and Sb 5p orbitals get heavily involved in those FM superexchanges, their strong SOC effects could also yield an exchange anisotropy as in CrI_3 [26,27].

We now identify each contribution of Cr, Sb, and Se elements to the MAE by performing LSDA+U+SOC calculations for the magnetization along the easy *a* or hard *b* axis. We first include the full SOC effect of the two elements, and tune the SOC effect of the third element from zero to its full value [see Fig. 7(a)]. The red, black, and blue curves mainly
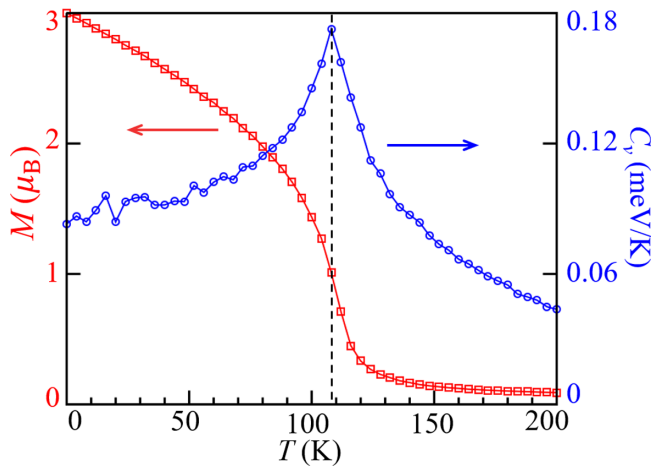
FIG. 8. Monte Carlo simulations of the magnetization and magnetic specific heat of CrSbSe₃ as a function of temperature. T_C is estimated to be 108 K.

show the respective contribution of Cr, Sb, and Se to the MAE, albeit their mutual enhancement. The Cr contribution is about 0.158 meV per atom and mainly the SIA type, and Sb (Se) is about 0.112 (0.048) meV per atom and mainly the EA type. It seems that the SIA and EA have almost equal contributions to the MAE. Second, we turn off the SOC effect of the two elements, and tune the SOC effect of the third element from zero to its full value [see Fig. 7(b)]. We see the Cr contribution of about 0.070 meV per atom to the SIA, and Sb (Se) contributions of 0.044 (0.012) meV per atom to EA, all of which are smaller than the corresponding contributions in the first case with a mutual enhancement of the SOC effects. These two sets of the results show that the SIA contribution from Cr and the EA one from Sb plus Se, are both moderate and each contributes about half of the MAE.

We now carry out Monte Carlo simulations to estimate the Curie temperature of the pseudo 1D FM semiconductor CrSbSe₃, using the above parameters of the magnetic exchange and anisotropy. The spin Hamiltonian is

$$H = \sum_k \sum_{i,j} \frac{J_k}{2} \vec{S_i} \cdot \vec{S_j} + \sum_i \left\{ D(S_i^c)^2 + E_n[(S_i^a)^2 - (S_i^b)^2] \right\}$$

$$= \sum_k \sum_{i,j} \frac{J_k}{2} \vec{S_i} \cdot \vec{S_j} + \sum_i D|\vec{S_i}|^2 \cos^2\theta$$

$$+ \sum_i E_n[|\vec{S_i}|^2 \sin^2\theta(\cos^2\phi - \sin^2\phi)],$$

where the first term stands for the isotropic Heisenberg exchange, the second term with D describes the longitudinal (c axis) anisotropy, and the last term with E_n represents the transverse (ab plane) anisotropy. The sum over i runs over all Cr³⁺ sites with $S = 3/2$ in the spin lattice, and j over the neighbors of each i with their FM couplings J_k ($k = 1$–4; see Fig. 4 and Table I). $D = -0.033$ meV and $E_n = -0.042$ meV

are calculated using the above MAE values in the FM ground state (see Fig. 6). The Metropolis method [30] and a $10 \times 10 \times 10$ spin lattice with the periodic boundary condition are used in our simulations. During the simulation steps, each spin is rotated randomly in all directions. At each temperature, we use 10^8 Monte Carlo steps per site to reach an equilibrium, and 1.2×10^8 steps per site for statistical averaging. The magnetic specific heat, at a given temperature, is calculated according to $C_v = (\langle E^2 \rangle - \langle E \rangle^2)/(k_B T^2)$, where E is the total energy of the spin system. The calculated magnetization and magnetic specific heat show that the Curie temperature is 108 K (see Fig. 8). Compared with the experimental T_C of 71 K, the present Monte Carlo simulations give an overestimated but reasonable T_C, without considering the phonon contribution and spin-phonon interaction. This is often the case in low-dimensional magnetic materials [19,20]. Overall, the present work reasonably accounts for the band gap and magnetic properties of this pseudo 1D FM semiconductor.

IV. CONCLUSIONS

In summary, we study the electronic structure and magnetic properties of the pseudo 1D FM semiconductor CrSbSe₃, using density functional calculations, superexchange model analyses, and Monte Carlo simulations. Our results show that CrSbSe₃ is a strongly covalent Mott-type semiconductor with a band gap of 0.65 eV and the total spin moment of 3μ_B/f.u. (from the formal Cr³⁺ $S = 3/2$ state), both of which well reproduce the experiments. We find two major FM couplings within the zigzag spin chain along the b axis, which are rationalized by the FM superexchange picture of the near-90° Cr-Se-Cr bonds, but the interchain FM couplings are one order of magnitude weaker, thus corroborating the pseudo 1D structure of CrSbSe₃. Moreover, our calculations reproduce the experimental easy magnetization a axis and the hard b axis, and we find that the single ion anisotropy from Cr and the exchange anisotropy from Sb plus Se have nearly equal contributions to the calculated magnetic anisotropic energy of 0.19 meV/Cr. Using the parameters of the magnetic exchange and anisotropy, our Monte Carlo simulations give the Curie temperature of 108 K. Overall, this work reasonably accounts for the magnetic properties of the pseudo 1D FM semiconductor CrSbSe₃.

Note added. Recently, we noticed a paper [31] which presents a theoretical study of the ferromagnetism for the hypothetical 1D spin chain of CrSbSe₃. Their results of the strong intrachain FM couplings are similar to ours for the real bulk material.

[1] B. Huang, G. Clark, E. Navarro-Moratalla, D. R. Klein, R. Cheng, K. L. Seyler, D. Zhong, E. Schmidgall, M. A. McGuire, D. H. Cobden, W. Yao, D. Xiao, P. Jarillo-Herrero, and X. Xu, Nature (London) **546**, 270 (2017).

[2] C. Gong, L. Li, Z. Li, H. Ji, A. Stern, Y. Xia, T. Cao, W. Bao, C. Wang, Y. Wang, Z. Q. Qiu, R. J. Cava, S. G. Louie, J. Xia, and X. Zhang, Nature (London) **546**, 265 (2017).

[3] K. S. Burch, D. Mandrus, and J.-G. Park, Nature (London) **563**, 47 (2018).

[4] M. A. McGuire, H. Dixit, V. R. Cooper, and B. C. Sales, Chem. Mater. **27**, 612 (2015).

[5] N. D. Mermin and H. Wagner, Phys. Rev. Lett. **17**, 1133 (1966).

[6] L. Landau and E. Lifshitz, in *Statistical Physics*, 3rd ed. (Butterworth-Heinemann, Oxford, 1980).

[7] P. Fazekas, *Lecture Notes on Electron Correlation and Magnetism* (World Scientific, Singapore, 1999).

[8] J. Zhang, X. Cai, W. Xia, A. Liang, J. Huang, C. Wang, L. Yang, H. Yuan, Y. Chen, S. Zhang, Y. Guo, Z. Liu, and G. Li, Phys. Rev. Lett. **123**, 047203 (2019).

[9] D. A. Odink, V. Carteaux, C. Payen, and G. Ouvrard, Chem. Mater. **5**, 237 (1993).

[10] V. Volkov, G. Van Tendeloo, J. Van Landuyt, S. Amelinckx, E. Busheva, G. Shabunina, T. Aminov, and V. Novotortsev, J. Solid. State. Chem. **132**, 257 (1997).

[11] T. Kong, K. Stolze, D. Ni, S. K. Kushwaha, and R. J. Cava, Phys. Rev. Mater. **2**, 014410 (2018).

[12] Y. Sun, Z. Song, Q. Tang, and X. Luo, J. Phys. Chem. C **124**, 11110 (2020).

[13] Y. Liu, Z. Hu, and C. Petrovic, Phys. Rev. B **102**, 014425 (2020).

[14] T. Mathew, S. Rahul K, and V. Mathew, Comput. Condens. Matter **23**, e00467 (2020).

[15] G. Kresse and J. Furthmüller, Phys. Rev. B **54**, 11169 (1996).

[16] G. Kresse and D. Joubert, Phys. Rev. B **59**, 1758 (1999).

[17] V. I. Anisimov, I. V. Solovyev, M. A. Korotin, M. T. Czyżyk, and G. A. Sawatzky, Phys. Rev. B **48**, 16929 (1993).

[18] V. I. Anisimov, F. Aryasetiawan, and A. I. Lichtenstein, J. Phys.: Condens. Matter. **9**, 767 (1997).

[19] Y. Guo, Y. Zhang, S. Yuan, B. Wang, and J. Wang, Nanoscale **10**, 18036 (2018).

[20] S. Chen, F. Wu, Q. Li, H. Sun, J. Ding, C. Huang, and E. Kan, Nanoscale **12**, 15670 (2020).

[21] H. Wang, J. Qi, and X. Qian, Appl. Phys. Lett. **117**, 083102 (2020).

[22] D. I. Khomskii, *Transition Metal Compounds* (Cambridge University Press, Cambridge, UK, 2014).

[23] H. J. Monkhorst and J. D. Pack, Phys. Rev. B **13**, 5188 (1976).

[24] J. Zaanen, G. A. Sawatzky, and J. W. Allen, Phys. Rev. Lett. **55**, 418 (1985).

[25] H. Wang, F. Fan, S. Zhu, and H. Wu, Europhys. Lett. **114**, 47001 (2016).

[26] J. L. Lado and J. Fernández-Rossier, 2D Mater. **4**, 035002 (2017).

[27] D.-H. Kim, K. Kim, K.-T. Ko, J. H. Seo, J. S. Kim, T.-H. Jang, Y. Kim, J.-Y. Kim, S.-W. Cheong, and J.-H. Park, Phys. Rev. Lett. **122**, 207201 (2019).

[28] K. Yang, F. Fan, H. Wang, D. I. Khomskii, and H. Wu, Phys. Rev. B **101**, 100402(R) (2020).

[29] L. Liu, K. Yang, G. Wang, and H. Wu, J. Mater. Chem. C **8**, 14782 (2020).

[30] N. Metropolis and S. Ulam, J. Am. Stat. Assoc. **44**, 335 (1949).

[31] Y. Xun, Z. Zhu, X. Chen, and J. Qi, Phys. Rev. B **104**, 085429 (2021).